Grinding Induced Changes in Residual Stresses of Carburized Gears

R. LeMaster, B. Boggs, J. Bunn, C. Hubbard and T. Watkins

Management Summary

This paper presents the results of a study performed to measure the change in residual stress that results from the finish grinding of carburized gears. Residual stresses were measured in five gears using the x-ray diffraction equipment in the Large Specimen Residual Stress Facility at Oak Ridge National Laboratory. Two of the gears were hobbed, carburized, quenched and tempered, but not finished. The remaining three gears were processed similarly, but were finish ground. The residual stresses were measured at 64 different locations on a tooth from each gear. Residual stresses were also measured at fewer points on other teeth to determine the tooth-to-tooth variation. Tooth profile measurements were also made of the finished and unfinished gear samples.

The results show a fairly uniform and constant compressive residual field in the non-finished gears. There was a significant reduction in the average residual stress measured in the finished gears. Additionally, there was a significant increase in the variability of the residual stress that was introduced by the grinding process. Large variations were observed in both the lateral and longitudinal directions on a tooth surface. Analysis of the data suggests a linear relationship between the change in average residual stress and the amount of material removed by the grinding process.

Introduction

Carburizing is a commonly used method for increasing the strength and wear resistance of gearing. A significant benefit of the carburization process is that compressive residual stresses are developed near the surface due to phase transformations that occur during the post carburization heat treatment steps. After carburization it is necessary to finish the gear by processes such as grinding or skiving. These finishing processes develop the precise geometric form required while improving the surface finish. Finishing processes change the residual stress imparted by carburization and subsequent heat treatment processes. These changes are due to the removal of material and the associated rebalancing of the residual stresses and the introduction of near surface residual stresses by the machining operations.

A grinding allowance is used to specify the amount of material to be left on a machined gear prior to heat treatment. This excess material and any material associated with a geometry change during heat treatment are removed by the finishing process. The magnitude of this grinding allowance will affect the strength, fatigue life and wear resistance of the finished gear because of its relationship to changes in the residual stresses. Removal of the excess material will also remove any retained austenite.

Test Gears

The three finished ground samples were designated as Finished 1, 2 and 3. The two remaining unfinished samples were designated as Unfinished 1 and 2. Each gear had 25 teeth; a diametral pitch of 4 teeth/inch; a pressure angle of 20 degrees; full radius fillets; no addendum modification; and a face width of 0.75". The gears were flat with no ribs, rims or other weight reduction features (Fig. 1).

The measurement of residual stresses in gear teeth using x-ray diffraction is complicated by the curvature of the involute and trochoid geometries, and the potential for interference of the incident or diffracted beam by adjacent teeth. The size of the gears used in this study was chosen so that the residual stresses could be measured over most of the tooth surface.

Most of the residual stresses measured were in the longitudinal direction of the gear tooth (Fig. 2). A few residual stress measurements were also made in the lateral direction. The 64 locations on a tooth from each sample where residual stresses were measured are shown in Figure 3. There are eight lateral locations associated with each radius. The lateral locations are spaced 0.079". Residual stress measurements were not made at the critical bending stress location in the fillet. This was due to the high curvature in the fillet area and interference with the incident or refracted beam path from adjacent teeth.

The gear blanks for each sample were taken from the same length of 8620H bar stock. The steps used in the fabrication of the samples are listed in Table 1. The time at temperature for the normalize, stress relief and defuse steps was based on 1-hour-per-inch of thickness. The carburization step was done using an 80–90% natural gas-derived endothermic gas atmosphere. Test slugs were pulled during the carburization step to verify an effective case depth of 0.030". The final surface hardness was determined to be within the range of 58–62 HRC. The finish grinding was done using a vitrified alumina grinding wheel on a CNC grinder.

The profiles of each sample were measured using a CMM at Oak Ridge National Laboratory. The profiles were measured at three lateral locations on each sample. There was no discernible difference between the three lateral measurements for each sample when the measurements were superimposed. The profiles measured at the first lateral location on the five samples are compared in Figure 4. There was virtually no discernible difference between the measured profiles of the samples designated Unfinished 1 and Unfinished 2. There was also little noticeable difference between the samples designated Finished 1 and Finished 2. However, the gear designated Finished 3 had noticeably more material removed at the tip than did gears Finished 1 and Finished 2. At the pitch circle, all of the finished samples were virtually the same.

Figure 5 shows the grind depth versus radius for each of the finished samples. The grind depth reported is the perpendicular distance from the unfinished profile to the finished profile (Fig. 6). The increased tip relief observed in the sample designated Finished 3 is quite noticeable. With the exception of the tip relief found in Finished 3, the grind depth is similar for all radii greater than the form radius. The material removed at the pitch circle by grinding ranged from

continued

Figure 1—A typical finished gear. This gear is designated Finished 1.

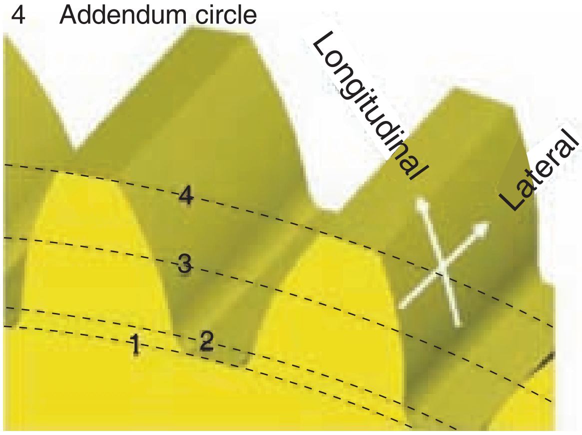

Figure 2—Longitudinal and lateral tooth directions on tooth.

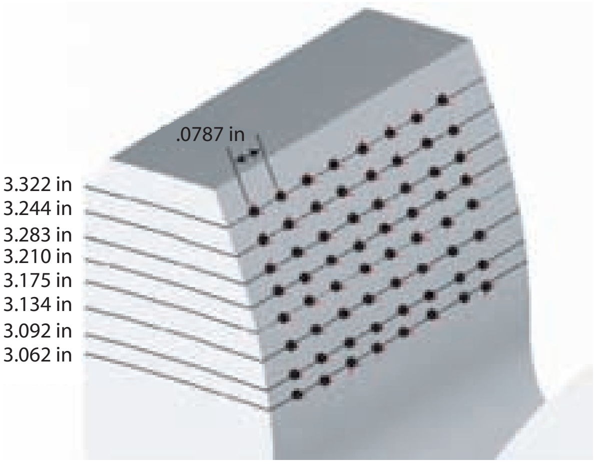

Figure 3—Radial and lateral locations where the residual stress measurements were made.

Table 1—Fabrication steps.

1.	Rough machine	
2.	Normalize	(1,740°F)
3.	Stress relief	(1,250°F)
4.	Finish machine	
5.	Carburize	(1,650°F)
6.	Defuse	(1,550°F)
7.	Oil quench	(135°F)
8.	Temper	(450°F)
9.	Finish grind	

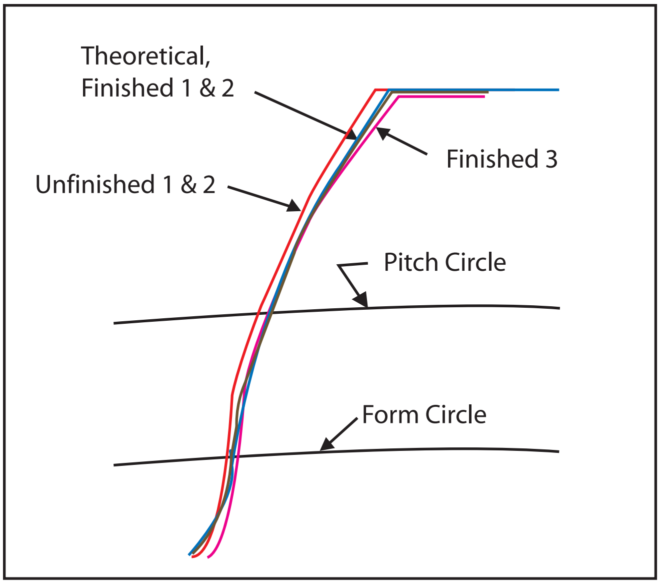

Figure 4—Comparison of the measurement profiles of the finished and unfinished gears.

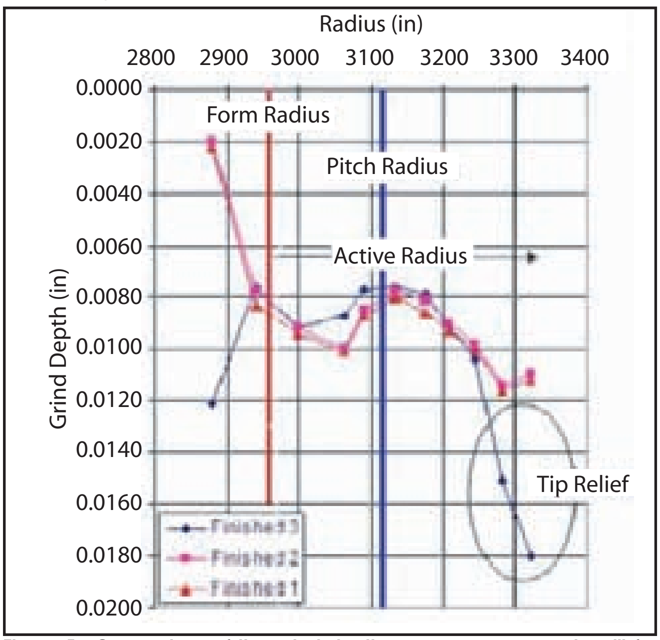

Figure 5—Comparison of the grind depth versus measurement radii for the three finished gears.

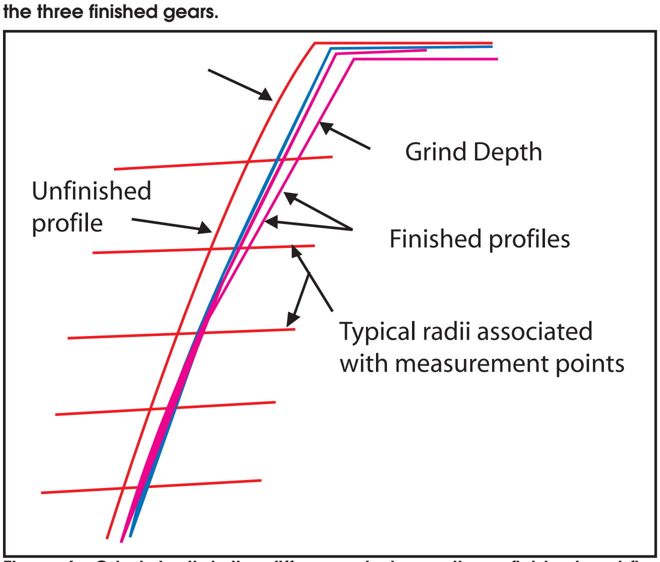

Figure 6—Grind depth is the difference between the unfinished and finished tooth surfaces measured normal to the finished gear tooth surface.

0.0082" to 0.0085" (0.208 to 0.216 mm).

X-Ray Diffraction Measurements

Residual stress measurements were made using the Model 1600 TEC diffractometer in the Residual Stress User Center at Oak Ridge National Laboratory. The residual stress measurements involved measuring the interatomic spacing (d-space) between atoms for the (211) crystal plane at different x-ray beam incident angles (ψ) (Ref.1). The measured d-space is the average value for a group of properly oriented grains near the irradiated surface. The residual stress was determined using the $\sin^2\psi$ technique (Ref. 2). In this method d-space is plotted as a function of $\sin^2\psi$. The y-intercept of the plot was taken as the unstrained d-space (d_0) with the slope being proportional to the residual stress. A 2 mm (0.079") diameter collimator, vanadium filter, and Kα radiation from a chromium x-ray target were used. Figure 7 shows a picture of a portion of the diffractometer and one of the samples mounted in the diffractometer. On average, 10 ψ-angles with a two-degree oscillation were used at each radial location. As seen in Figure 7, black electrical tape was used to cover neighboring teeth to eliminate any radiation scattered from them. Figure 8 provides an example of a typical d-space versus $\sin^2\psi$ plot.

Residual Stress Data for Unfinished Samples

The residual stress component acting in the longitudinal direction for the gears designated as Unfinished 1 and Unfinished 2 is shown in Figures 9 and 10. Each line is associated with a specific radius. There are eight data points per line. Table 2 gives the average and standard deviation of the longitudinal residual stress measured on the randomly selected tooth for each gear. The average and standard deviation values given in Table 2 are for the 64 measurement locations on the tooth.

The average residual stress for all 64 locations on the tooth from sample Unfinished 1 is 185 ksi and 150 ksi for Unfinished 2. The 35 ksi difference in the average longitudinal residual stress led to the measurement of the longitudinal residual stress at a similar location on several additional teeth of gear Unfinished 2. The tooth-to-tooth variation in the longitudinal residual stress (measured at a radius of 3.244" (82.4 mm) and lateral location of 0.315" (8 mm) is shown in Figure 11. The tooth-to-tooth variation ranges from 138 ksi to 191 ksi with an average value of 160 ksi. The average longitudinal residual stress measured on the tooth from both Unfinished 1 and Unfinished 2 fall within this tooth-to-tooth variation. Variations in residual stresses can be caused by non-homogeneous chemistry and microstructure in the material as well as non-uniform furnace heating, carbon potential and quenching rates.

The residual stress in the lateral direction was also measured at a few locations on the unfinished samples. The residual stresses were in all cases compressive and approximately equal to the residual stress measured in the longitudinal direction. This indicates a biaxial stress field in which the normal stresses were approximately equal. No

continued

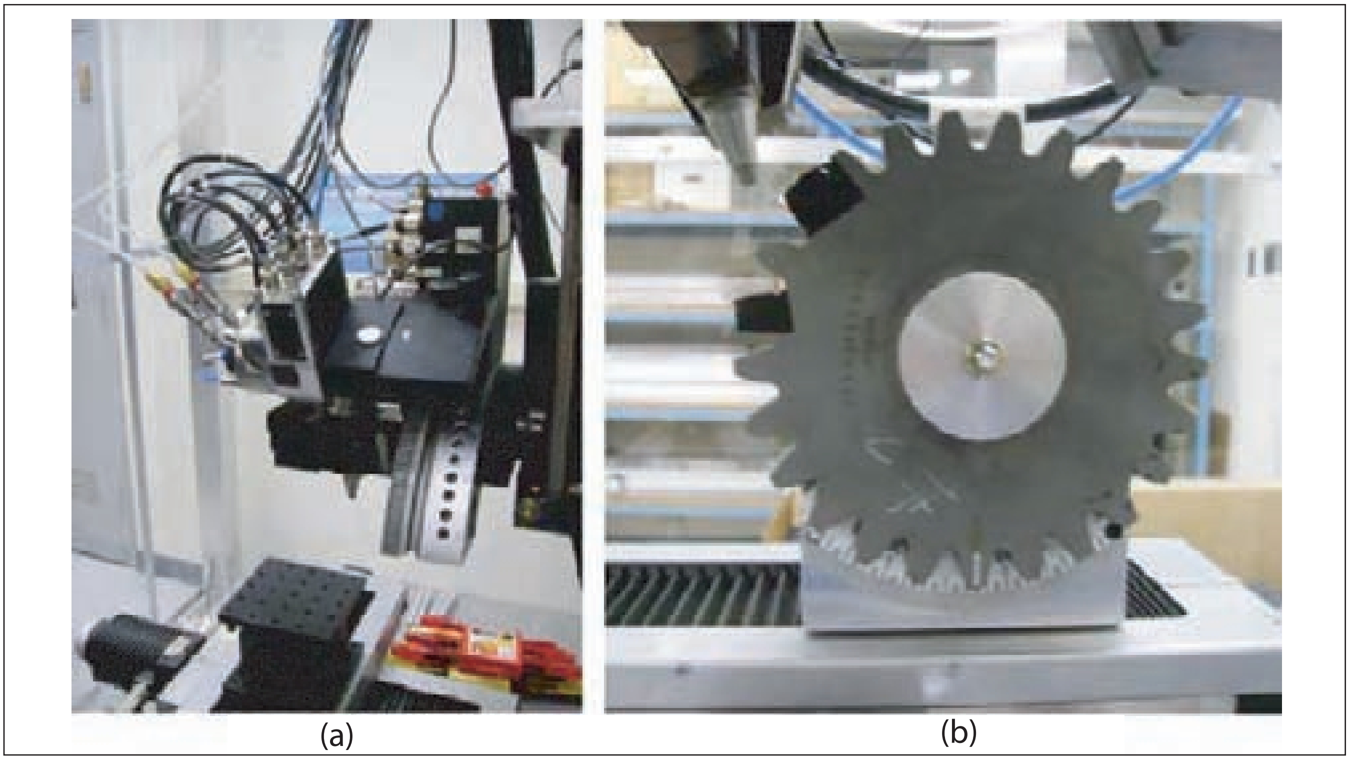

Figure 7—(a) X-ray source and detector portion of TEC model 1600 diffractometer; (b) Unfinished 2 mounted in x-ray diffractometer.

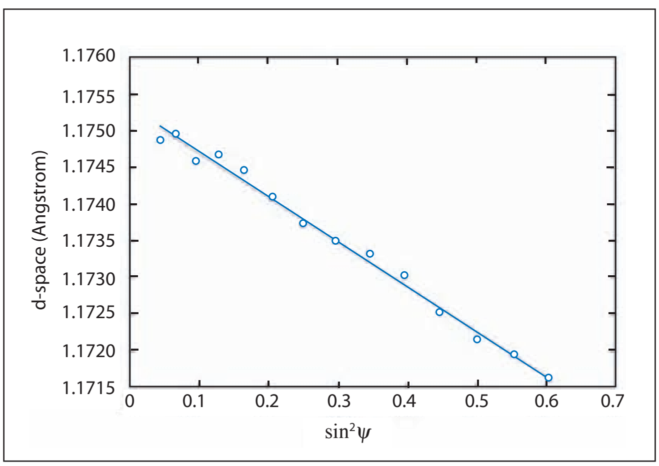

Figure 8—An example $\sin^2\psi$ plot used to determine the residual stress. The slope is proportional to the residual stress.

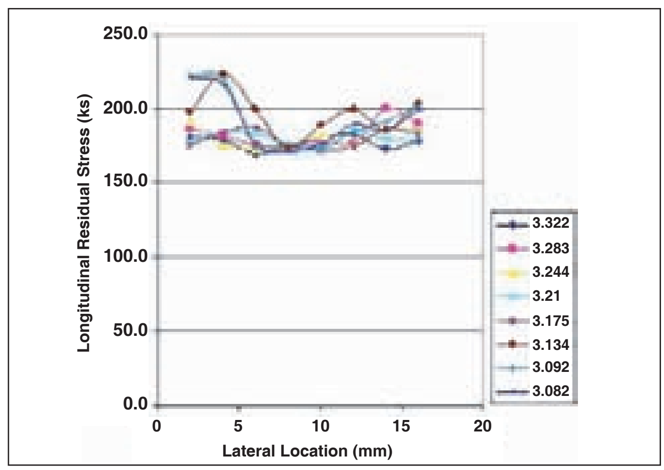

Figure 9—Longitudinal component of residual stress measured in gear Unfinished 1. Average = 185 ksi, Std. Dev. = ± 13 ksi.

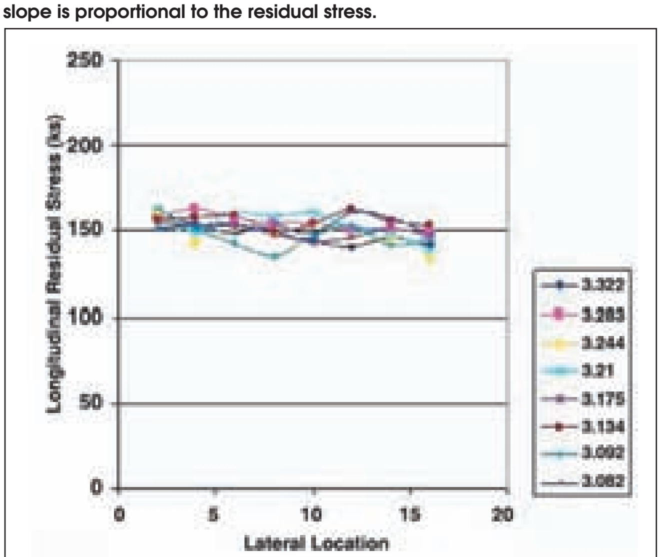

Figure 10—Longitudinal component of residual stress measured in gear Unfinished 2. Average = 150 ksi, Std. Dev. = ± 7 ksi.

Table 2—Statistical properties of longitudinal residual stress measurements.

Gear	Average longitudinal residual stress (ksi)	Standard deviation of longitudinal residual stress (ksi)
Unfinished 1	185	± 13
Unfinished 2	150	± 7
Finished 1	116	±15
Finished 2	108	±15
Finished 3	110	± 22

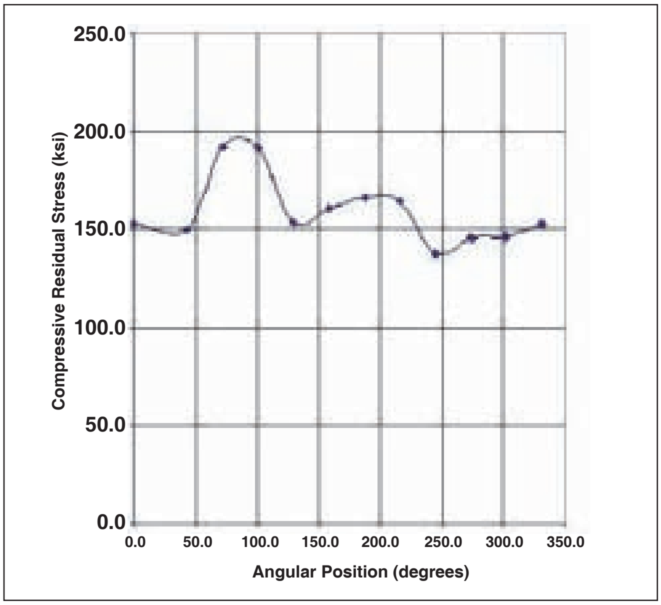

Figure 11—Tooth-to-tooth variation in the longitudinal residual stress measured at a radius of 3.244 inches and a lateral position of 0.315 inches. Average 160 ksi, Std. Dev. = ± 17 ksi.

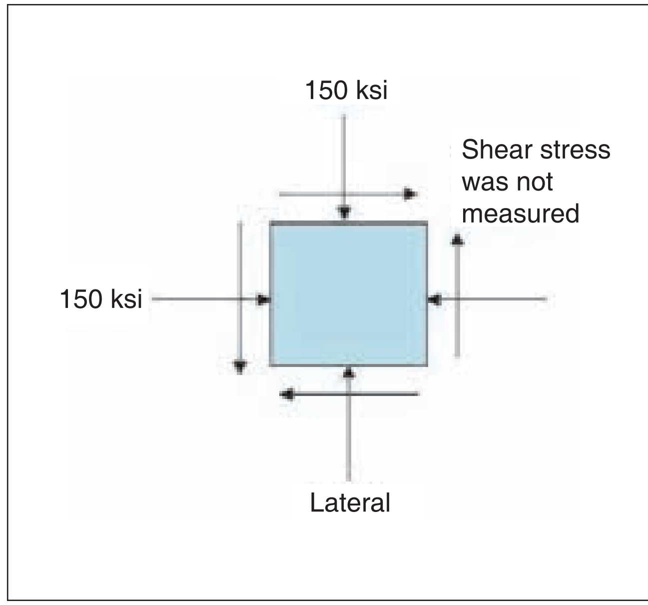

Figure 12—The unfinished gears exhibited a biaxial stress state with equal lateral and longitudinal compressive stresses.

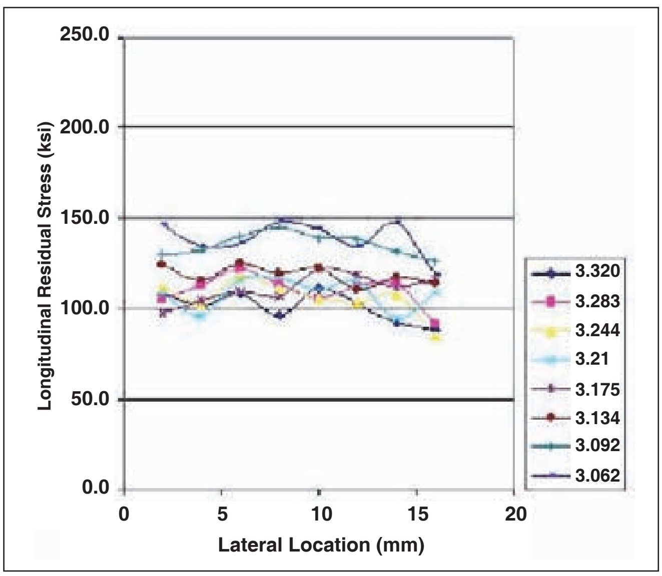

Figure 13—Longitudinal component of residual stress measured in gear Finished 1. Average = 116 ksi, Std. Dev. = ± 15 ksi.

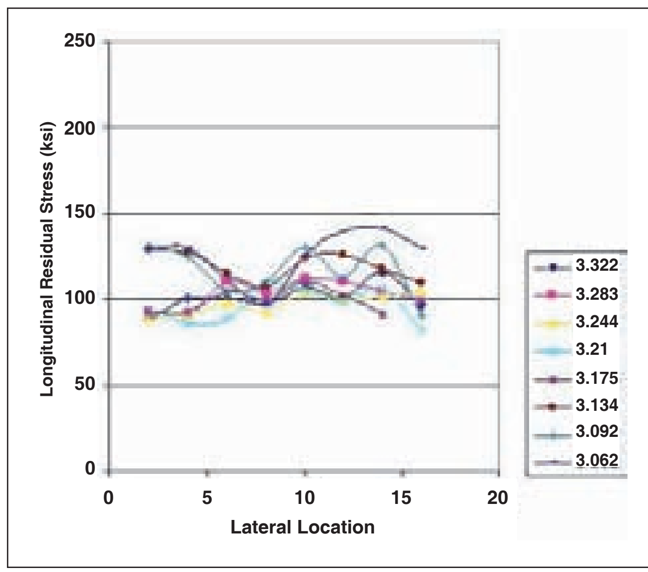

Figure 14—Longitudinal component of residual stress measured in gear Finished 2. Average = 108 ksi, Std. Dev. = ± 15 ksi.

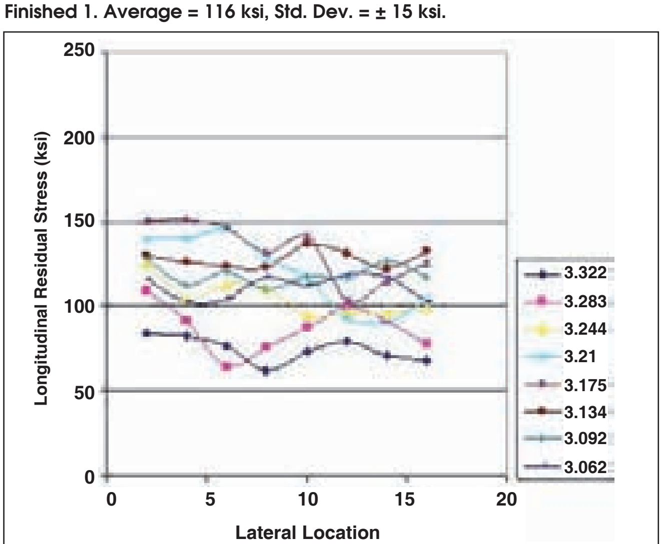

Figure 15—Longitudinal component of residual stress measured in gear Finished 3. Average = 108 ksi, Std. Dev. = ± 22 ksi.

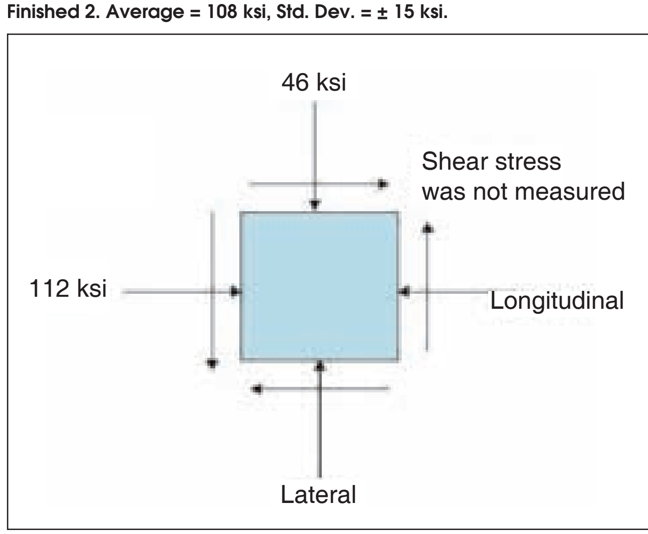

Figure 16—The finished gears exhibited a biaxial stress state with non-equal lateral and longitudinal compressive stresses. Data from gear Finished 1, tooth 1, lateral position 0.315 inch and radius of 3.244 inch.

shear stresses were measured. An example of the stress state for one of these points is shown in Figure 12.

Residual Stress Data for Finished Samples

The longitudinal residual stress measured on a randomly selected tooth on gears Finished 1, Finished 2 and Finished 3 is shown in Figures 13, 14 and 15. A comparison of these figures with Figures 9 and 10 shows that the finished gears have more variation than the unfinished gears. Table 2 gives the average and standard deviation of the longitudinal residual stress for each gear. The average longitudinal residual stress in the finished gears is approximately the same with a maximum difference of 8 ksi. The standard deviations of the data are approximately the same for gears Finished 1 and Finished 2. The standard deviation of the longitudinal residual stress in Finished 3 is ± 22 ksi, which is considerably greater than that for Finished 1 (± 15) and Finished 2 (±15). This larger standard deviation is due in large part to the lower residual stresses measured at locations having a radius of 3.322" and 3.283" (bottom two lines of data in Figure 15). These lower residual stresses are expected due to a larger amount of material having been removed at the tooth tip.

The residual stress in the lateral direction was also measured at a few locations on the finished samples. Unlike the unfinished gears, the lateral residual stresses measured in the finished gears were different than those measured in the longitudinal direction. Figure 16 shows the stress state measured at a typical point. No shear stresses were measured.

Residual Stress Change versus Grind Depth for Gears Finished 1, 2 and 3

The eight residual stress measurements taken at each radial location were used to compute an average residual stress at each radius. These average residual stresses were then plotted on the same graph (different y-axes) with the grind depth. These plots are shown in Figures 17, 18 and 19. Note that the shape of the average residual stress curves is similar for gears Finished 1 and Finished 2, and grind depths are virtually identical.

However, the grind depth curves and the average residual stress curves have different shapes. The average residual stress curves have a negative slope and slight concave up appearance. The grind depth curves have a more concave down appearance. In contrast, the shapes of the average residual stress and grind depth curves for gear Finished 3 are similar. This suggests that there is a stronger correlation between grind depth and average residual stress in Finished 3 than there is in Finished 1 and Finished 2.

An analysis of the data presented in Figures 9, 10 and 11 suggests that the average longitudinal residual stress on the teeth of the unfinished gears is around 160 ksi. This is the average residual stress for the tooth-to-tooth data shown in Figure 11. Figure 9 and particularly Figure 10 also show that most of the measured residual stresses have limited variability. The change in residual stress due to the finish grinding was

continued

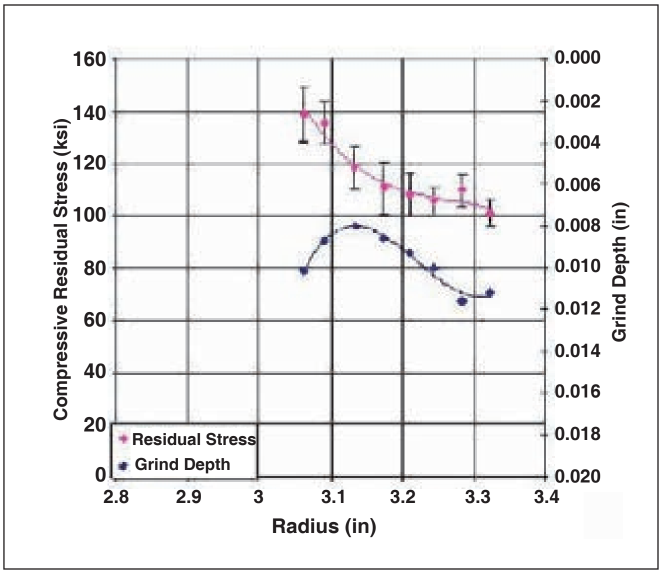

Figure 17—Average longitudinal residual stress and grind depth as a function of measurement radius for gear Finished 1.

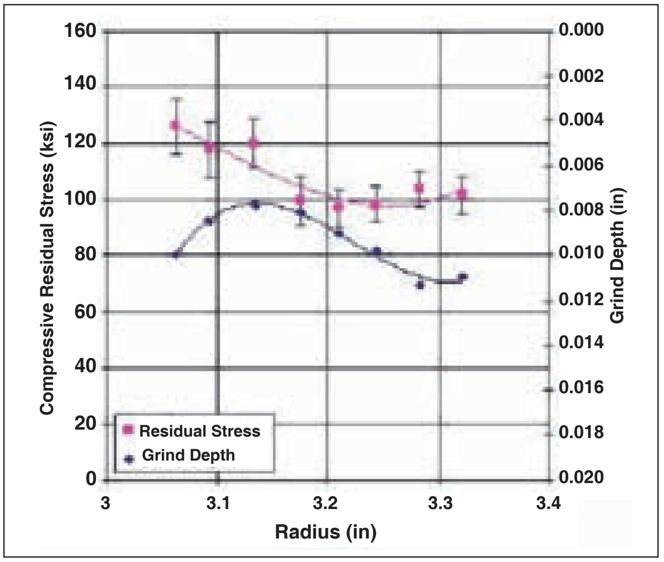

Figure 18—Average longitudinal residual stress and grind depth as a function of measurement radius for gear Finished 2.

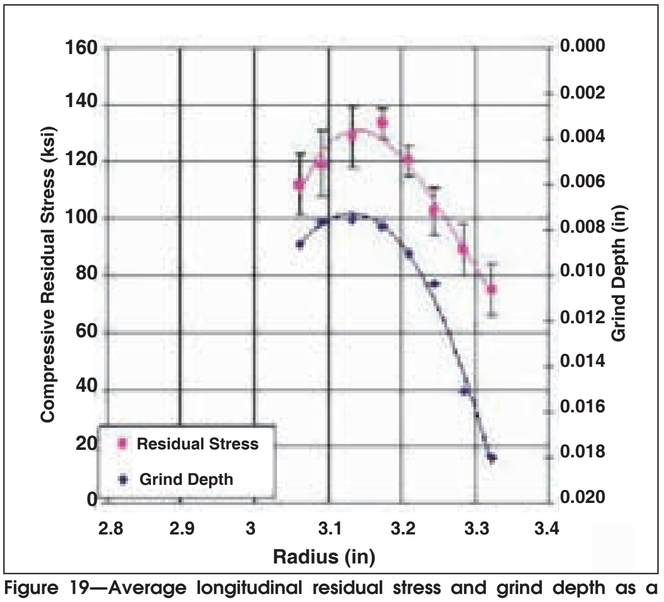

Figure 19—Average longitudinal residual stress and grind depth as a function of measurement radius for gear Finished 3.

computed as the difference between 160 ksi and the average residual stress at each radial location in the finished gears. This change in residual stress was then plotted versus grind depth and is shown in Figures 20, 21 and 22 for the three finished gears.

In each of these figures the linear curve fit is forced to pass through the origin so that at zero grind depth there is zero change in residual stress. Six of the eight data points for gear Finished 1 (Fig. 20) fall close to the linear line, which suggests a linear relationship between the change in residual stress and grind depth. There is more scatter in the data for gear Finished 2 (Fig. 21) and the linear relationship is not as evident. The data for Finished 3 (Fig. 22) also falls close to the linear line, which again suggests a linear relationship between the change in residual stress and grind depth.

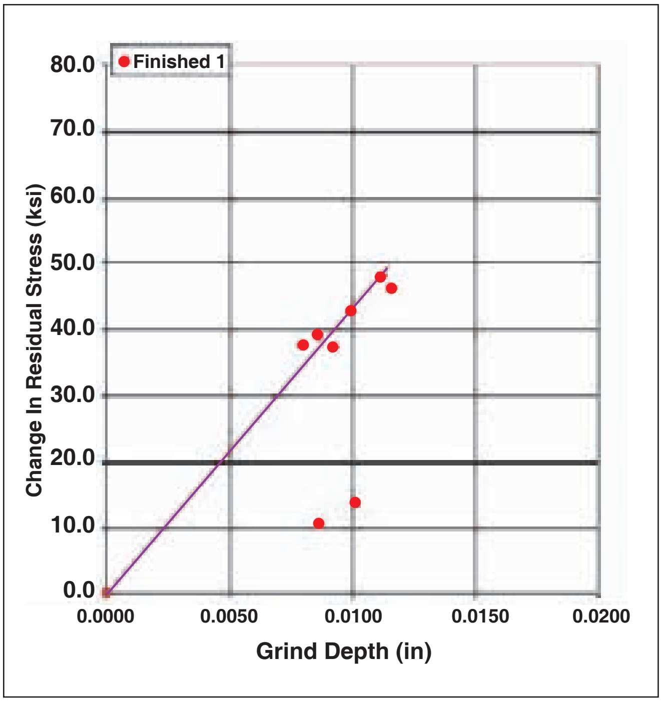

Figure 20—Change in the longitudinal component of residual stress as a function of grind depth for gear Finished 1.

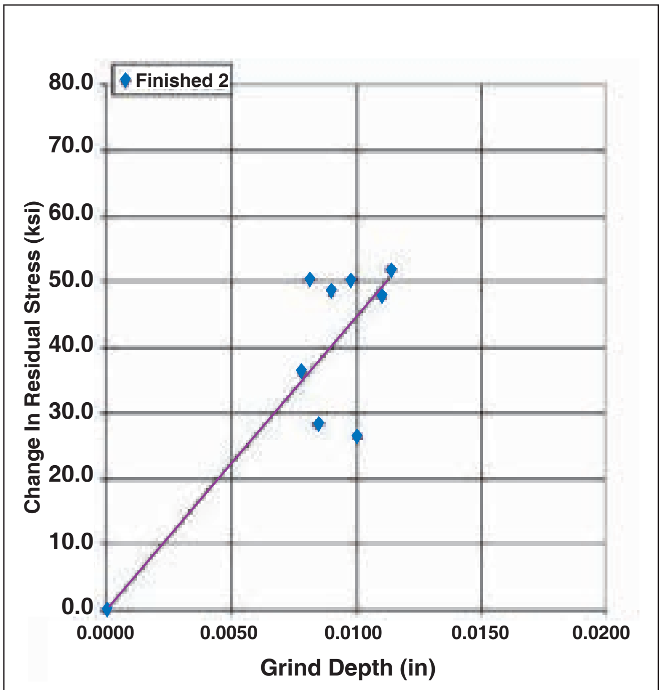

Figure 21—Change in the longitudinal component of residual stress as a function of grind depth for gear Finished 2.

Figure 23 is a composite graph that presents the change in residual stress versus grind depth data for all three of the finished gears. In this figure, 67% of the data shows good correlation with a linear relationship between change in residual stress and grind depth. 33% of the data points do not correlate as well with a linear relationship and suggest that at these locations there are other factors besides grind depth that are contributing to the change in residual stress. The equation for the linear regression line used to fit the data in Figure 23 is:

$$\Delta\sigma_R = 3{,}990 \cdot \delta,$$

where $\Delta\sigma_R$ is the change in the longitudinal component of the residual stress in ksi and δ is the grind depth in inches. As an example application of this equation, the change in residual stress due to a grind depth of 0.008" would be 32 ksi. Using 160 ksi as the initial residual stress in the unfinished gear, the residual stress in the finished gear would be reduced to 128 ksi. The applicability of this equation to gears other than the ones used in this study has not been established.

Conclusions

This paper presents the results of a study directed at measuring and quantifying the change in residual stress in carburized gears as a function of the amount of material removed during finish grinding. It is recognized that material removal is not the only mechanism by which residual stresses will change during the grinding process. Grinding itself will impose near surface residual stresses that could mask the effects of material removal. The data indicate that the grinding increased the variability in the residual stress measurements made on the finished gears as compared to the unfinished gears. The grinding also created a difference between the lateral and longitudinal components of the residual stress.

The data suggest that a linear equation may describe the relationship between change in residual stress and grind depth. The word "suggest" is used because not all of the data are served well by a linear equation. Whether the relationship between grind depth and change in residual stress is linear or not, the data show that decreasing grind depth will result in higher compressive residual stresses. The higher residual stresses should yield an increase in strength, life and wear resistance. In the specimens used in this study, an average reduction of 40 ksi was observed in the longitudinal component of residual stress. This average value is associated with a grind depth of 0.009". A maximum reduction of 75 ksi was also observed at a grind depth of 0.018", which occurred at the tip of gear Finished 3.

A large number of measurements were made in this study to determine the variation of residual stresses on the surface prior to and after finish grinding. The finished gears exhibited more variation than did the unfinished gears. As an example of the range of values that can exist, the longitudinal residual stress component ranged from 62.6 ksi to 151 ksi for gear Finished 3, and from 173 ksi to 224 ksi for Unfinished 1. Therefore, residual stresses should not be thought of as being the same at all locations on the surface of a tooth.

Acknowledgments

Gear samples used in this study were provided by B&R Machine & Gear, Sharon, TN.

This research was supported by the Department of Energy's Faculty and Student Team program at Oak Ridge National Laboratory, the Stanley Jones Professorship and the Office of Research, Grants and Contracts at the University of Tennessee at Martin.

This research was also sponsored by the Assistant Secretary for Energy Efficiency and Renewable Energy, Office of Freedom CAR and Vehicle Technologies, as part of the High Temperature Materials Laboratory User Program, Oak Ridge National Laboratory, managed by UT-Battelle, LLC, for the U.S. Department of Energy under contract number DE-AC05-00OR22725.

References

1. Noyan, I.C. and J.B. Cohen. *Residual Stress: Measurement by Diffraction and Interpretation*, Springer-Verlag, New York, 1987.
2. Cullity, B.D. and S.R. Stock. *Elements of X-Ray Diffraction*, 3rd Ed., Prentice-Hall, 2001.

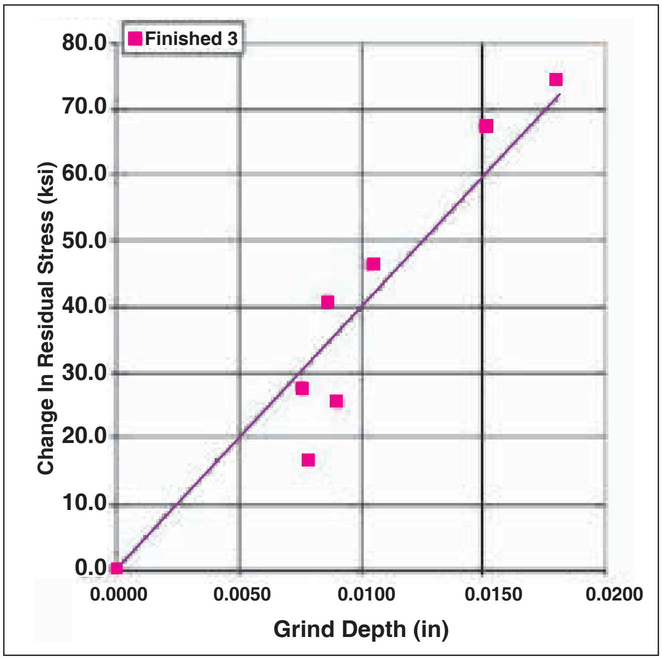

Figure 22—Change in the longitudinal component of residual stress as a function of grind depth for gear Finished 3.

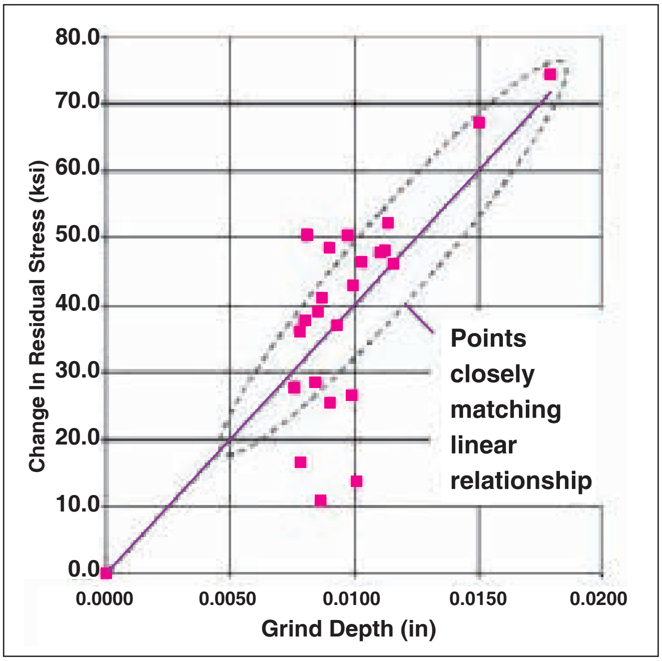

Figure 23—Composite graph showing the change in the longitudinal component of residual stress vs. grind depth for all three finished gears.

Bryan Boggs *in 2007 received a bachelor's degree in engineering with a specialty in mechanical engineering from the University of Tennessee at Martin. He was the recipient of the Outstanding Upper Division Engineering Student Award at UT Martin in 2007.*

Jeffrey Bunn *graduated from the University of Tennessee at Martin with a bachelor's degree in engineering and a concentration in civil engineering in May 2007. He is currently a doctoral student in the civil engineering department at the University of Tennessee Knoxville. His research is in the pairing of neutron diffraction and neutron imaging techniques to characterize hydrogen fuel cells. He is an IGERT fellow on the STAIR (Sustainable Technology through Advanced Interdisciplinary Research) program at UT Knoxville.*

Camden R. Hubbard *is a distinguished R&D staff member—Material Science and Technology Division—at Oak Ridge National laboratory, Oak Ridge, TN. Hubbard received a doctorate in physical chemistry at Iowa State University in 1971 and a bachelor's degree from the University of California, Berkeley in 1966. He leads the ORNL Diffraction and Thermophysical Properties Group and the Residual Stress User Center of the High Temperature Materials Laboratory. He previously served at NBS (now NIST) and developed there the Standard Reference Materials and Reference Data for X-ray, and he led programs for reference data on advanced ceramics. Hubbard has published over 200 papers, is past chairman of the International Centre for Diffraction Data and a distinguished fellow there since 2006. He has been an ACerS member for over 25 years and a member of the Basic Sciences and Engineering Ceramics Division.*

Dr. Robert Le Master *is a professor in the department of engineering at the University of Tennessee at Martin, where he teaches courses in the general areas of machine design and materials science. His research interests lie in carburization processes and associated residual stresses. Prior to entering academia, he worked in the aerospace industry, where he contributed to NASA and U.S. Air Force projects. He is the recipient of the Stanley Jones Professorship at UT Martin and is the recipient of several teaching awards.*

Thomas R. Watkins *is a senior research staff member in the Materials Science and Technology Division at the Oak Ridge National Laboratory (ORNL). He graduated with a bachelor's in ceramic engineering from Alfred University, and a master's and doctorate in ceramic science from The Pennsylvania State University. Upon finishing graduate school, he joined ORNL in 1992. His research interests include residual stresses, x-ray and neutron diffraction and mechanical properties of materials—particularly related to the understanding of the relationships between the macroscopic and crystallographic responses of materials during loading. He has co-authored more than 40 journal publications.*